AD-A193 430 MINIATURE RESPIRATORY SENSOR(U) HIGH TECHNOLOGY SENSORS 1/1
INC LONGWOOD FL FEB 88 N00014-87-C-0765

UNCLASSIFIED F/G 23/5 NL

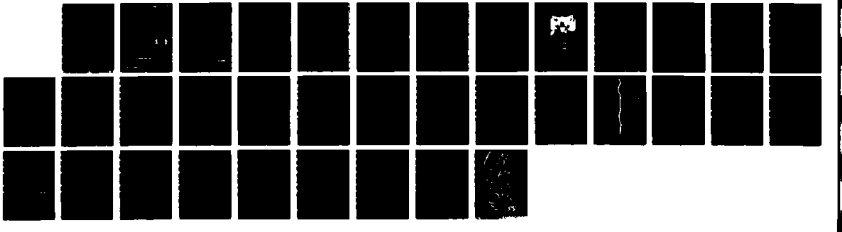

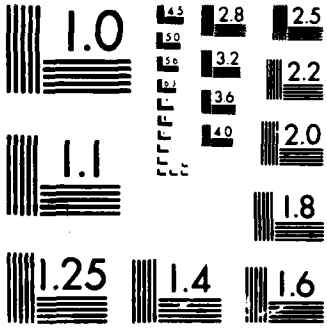
1.0
1.1
1.25
1.4
1.6
1.8
2.0
2.2
2.5
2.8
3.2
3.6
4.0
4.5
5.0
5.6

MINIATURE RESPIRATORY SENSOR

CONTRACT NO. N00014-87-C-0765

FINAL REPORT

August, 1987 through January, 1988

Prepared By

HIGH TECHNOLOGY SENSORS, INC.
262 EAST HORNBEAM DRIVE
LONGWOOD, FLORIDA 32779

February, 1988

SCIENTIFIC OFFICER
LCDR. GUY R. BANTA (CODE NMRDC-404)
NMCNCR, BETHESDA, MARYLAND 20814-5044

[redacted]

CONTRACT NO. N00014-87-C-0765
CONTRACTOR: HIGH TECHNOLOGY SENSORS, INC.

TECHNICAL ABSTRACT

A miniature Non-Dispersive Infrared (NDIR) sensor suitable for incorporation within the oxygen mask of an aviator has been demonstrated. The sensor utilizes a miniature infrared source. Current is injected into the source in order to alter its' emissivity to produce modulated infrared output. The source was modulated at 2.3 KHz and its' output focused on a cooled lead selenide detector. Data was taken demonstrating the capability of the sensor to detect expired carbon dioxide profiles in a breath by breath manner.

PROGRAM SUMMARY

The feasibility of utilizing a miniature NDIR sensor within an aviator's oxygen mask has been demonstrated. A breadboard sensor was designed, fabricated and evaluated. The sensor provided carbon dioxide concentration data suitable for breath by breath analysis.

The sensor contains a solid state source that is electronically modulated at 2.3 KHz, infrared optics, and a cooled solid state detector. The power dissipation and noise of the breadboard sensor were measured. Additional tests were performed on the effects of high humidity on the sensor.

An evaluation was made of the broadening effects of nitrogen and oxygen on the absorption characteristics of carbon dioxide. Tests were also conducted on a miniature flow sensor to determine its' suitability for incorporation within the respiratory sensor.

TABLE OF CONTENTS

LIST OF FIGURES

LIST OF TABLES

I. INTRODUCTION

This report summarizes the activities of Contract N00014-87-C-0765 for the period of August 1, 1987 through January 31, 1988. The purpose of the program was to determine the feasibility of fabricating a miniature respiratory sensor using Non-Dispersive Infrared (NDIR) technology which could be incorporated within an aviator's oxygen mask.

The activities in Phase I included sensor modeling, the design, fabrication and evaluation of a breadboard sensor, broadening tests and engineering analysis.

The completed breadboard assembly is pictured in Figure 1. The breadboard was designed to be incorporated in line within the MBU-12/P oxygen mask assembly. One end of the sensor assembly attaches to the hardshell of the mask. The valve assembly attaches to the other end. The sensor was designed for minimum restriction of the airway. The extension of the assembly provides for space around the airway for electronics.

The key elements of the breadboard sensor are a solid state infrared (IR) source, miniature optics, an interference filter and an IR detector. The radiation from the source is guided through a sensing chamber and focused onto a detector. Carbon dioxide passing through the chamber absorbs the radiation causing the detector to generate a signal. Sensor electronics amplify the detector signal.

This report contains a discussion of the breadboard sensor design, data on the testing of the breadboard sensor, data on broadening tests, conclusions and recommendations.

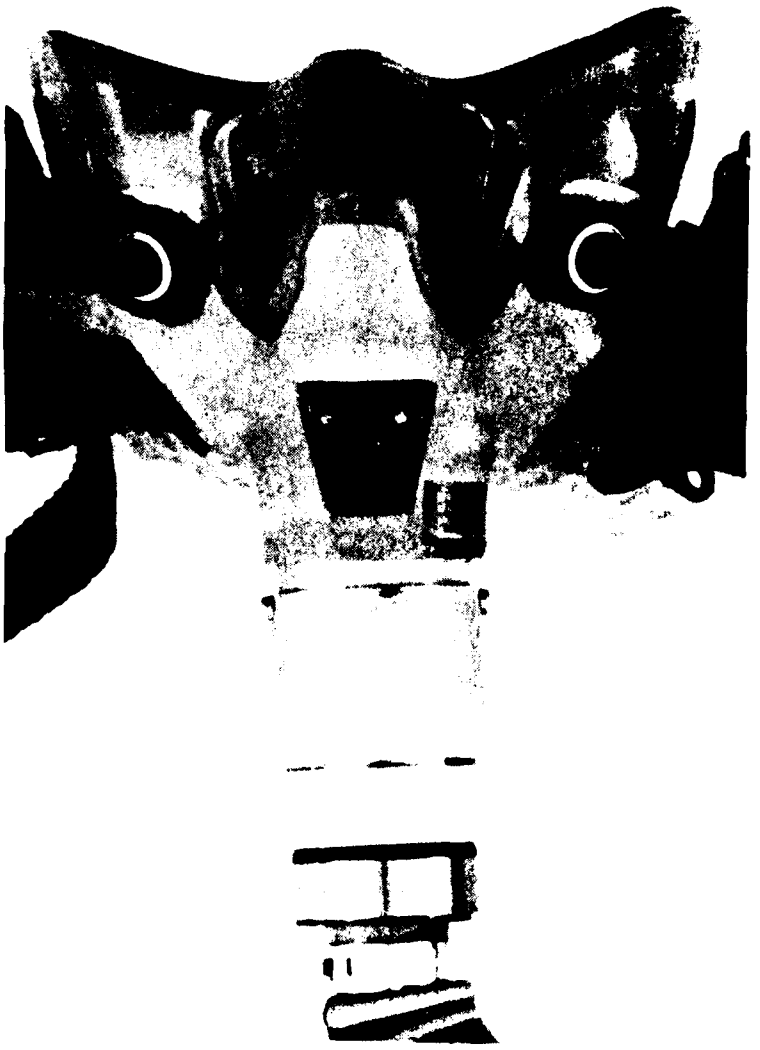

Figure 1. Breadboard Sensor

II. BREADBOARD DESIGN

Numerous techniques exist for the measurement and monitoring of gases (1) (2) (3). Some sensors react chemically with the gas in order to produce a visually observable effect. Other sensors measure an electronic signal generated by a electrochemical reaction with the gas or a change that occurs in the dielectric, electrical, or optical characteristics of a film exposed to a gas. More complex systems utilize gas chromatography and mass spectroscopy in order to separate, measure and identify various gaseous components.

Non-Dispersive Infrared (NDIR) techniques rely upon the measurement of optical transmission of gases in the infrared. The technique is widely used for medical applications because of its' speed and accuracy. Non-symmetric gas molecules absorb radiation in the infrared spectrum. The amount of absorption depends upon the molecular structure, the background gases and the concentration of the gas. The absorption characteristics vary as a function of wavelength allowing the sensors to be designed for specific gases. These absorption characteristics are well known (4) (5).

A simple NDIR sensor is shown in Figure 2. The sensor is composed of an infrared source, a gas cell which contains the gas to be analyzed and a detector. Optics focus the radiation generated by the source through the gas cell onto the detector. A mechanical chopper/filter wheel is used to filter radiation for the desired wavelength and to modulate the radiation.

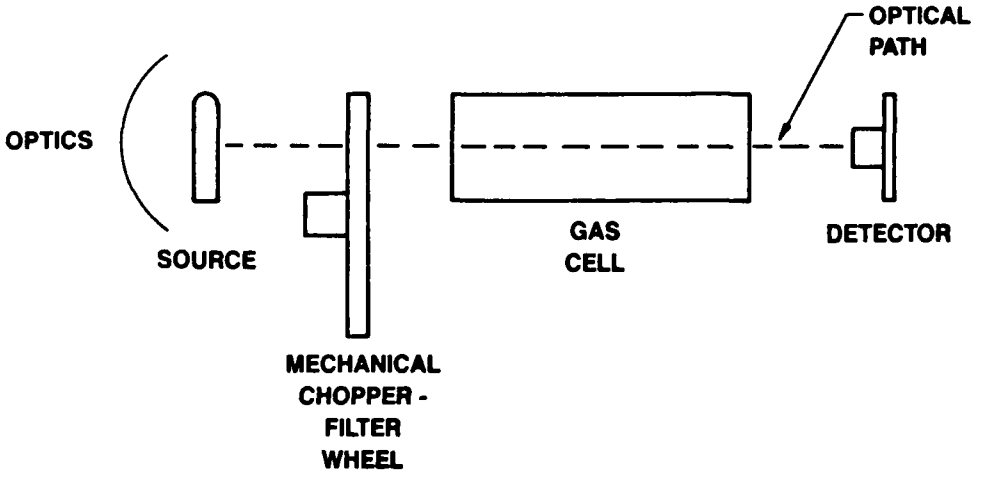

Figure 2. Conventional NDIR Gas Sensor

In general the signal level to be detected is small i.e., a few microvolts. The chopper provides modulation that overcomes problems with electronic drift which can obscure low level signals. The source and the detector also have characteristics that change with temperature. Some sensors employ a technique that alternately focuses radiation through the measuring cell then a reference cell containing a known gas concentration in order to compensate for temperature effects.

The breadboard sensor to be used for sensing respiratory functions has been designed using the EKLP source developed by High Technology Sensors (6). The source is small in size, and modulation of infrared output is obtained electronically. The small size and low power requirement of the source make it possible to develop a NDIR sensor which can be located within a pilot's oxygen mask.

The basic structure of the source is illustrated in Figure 3. A semiconductor is heated to the desired operating temperature. This is accomplished by mounting the semiconductor atop a thermal insulator and attaching a heater and temperature sensor to the semiconductor. The semiconductor will emit radiation according to the Planks' Law provided in Equation 1.

Equation 1: $E = \varepsilon\varepsilon_0\sigma T^4 A$

Where
- E = Emittance
- ε = Semiconductor emissivity
- ε_0 = Emissivity of free space
- σ = Boltzman's constant
- T = Temperature
- A = Area of emitting surface

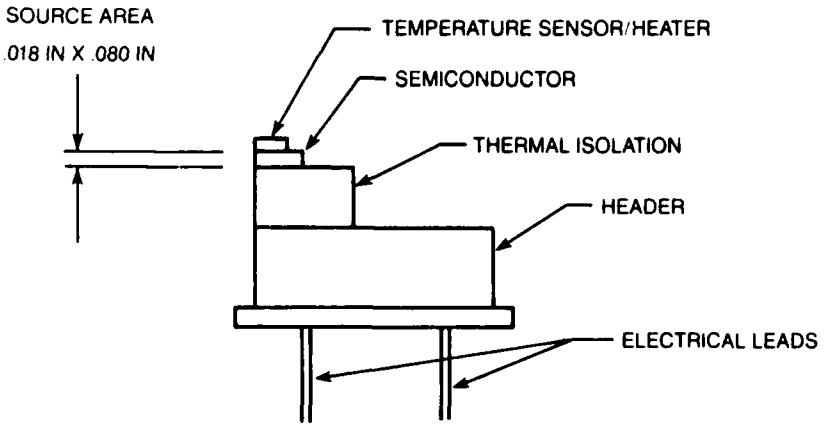

Figure 3. Basic Structure of EKLP Source

Excess carriers injected into the semiconductor will modulate the emissivity of the semiconductor in the infrared allowing modulated IR radiation to be produced.

The amount of radiation reaching the detector depends upon source temperature, optics, optical filter characteristics gas pathlength and operating wavelengths. Models developed by High Technology Sensors were used to evaluate the appropriate pathlength and the necessity for optics within the sensor.

The sensitivity of the sensor is given as the ratio of the detector output when no gas is present minus the detector output when a given percentage of gas is present in the sensor to the detector noise. The output of the detector will be the product of its' responsivity and the optical power reaching the detector. Hence, the sensitivty can be expressed as in Equation 2.

Equation 2:

$$S = \frac{R(P_0 - P_1)}{N_0}$$

S	=	Sensitivity
R	=	Detector Responsivity
N_0	=	Detector Noise
P_0	=	Modulated Optical Power on Detector Without Gas
P_1	=	Modulated Optical Power on Detector with Gas in Sensing Chamber

The optical power on the detector is modeled as the summation of power within small wavelength increments within the optical band of interest. Equation 3 defines the equation used to determine the power on the detector.

Equation 3:

$$P = \sum_{\lambda_1}^{\lambda_2} \Delta E(\lambda)\, \Phi(\lambda)\, \Gamma_{Gas}(\lambda)\, \Gamma_{Fil}(\lambda)\, \Delta\lambda$$

where:

$\Phi(\lambda)$	=	Optical Transfer Coefficient (considers source geometry and optics)
$\Delta E(\lambda)$	=	Modulated emittance at λ of source for interval $\Delta\lambda$
$\Gamma_{Gas}(\lambda)$	=	Gas transmittance through sample chamber at λ
$\Gamma_{Fil}(\lambda)$	=	Interference filter transmission at λ
λ_1, λ_2	=	Band limits

Further definitions of the individual components of the model depend upon the absorption band of the gas to be sensed. Carbon dioxide has a major absorption peak in the infrared at 4.3 microns. The gas transmission in the band will be modeled by the strong line Elsasser Model (7) defined by Equation 4.

Equation 4: $\Gamma_{Gas}(\lambda) = 1 - \text{erf}[(.5\beta^2\psi)^{1/2}]$

where
- ψ = a line strength variable characteristic of the gas at a given λ
- β = a variable primarily dependent upon path length and gas concentration

A graph of the calculated transmission characteristics for various path lengths at a concentration of 4% CO2 are provided in Figure 4. The variations in transmission as a function of pathlength although nonlinear are repeatable. Similar variations occurs with concentrations and a one to one correspondence can be made between transmission and concentrations for a given pathlength.

Although the total source emittance is defined by Equation 1 the emittance within a given optical band is more complicated. The modulated source emittance in the model is determined by an infinite series (7) given by Equation 5.

Equation 5: $\Delta E(\lambda) = \Delta\epsilon A M_{\Delta\lambda}$

where
- $\Delta\epsilon$ = Emissivity difference of source
- A = Source area

and where $M_{\Delta\lambda} = 8.73 \times 10^{-13} T^4 \Sigma_1$

and
$$\Sigma_1 = \sum_{m=1}^{\infty} e^{-u_2 m} m^{-4}(u_2^3+3u_2^2+6u_2+6) = \sum_{m=1}^{\infty} e^{-u_1 m} m^{-4}(u_1^3+3u_1^2+6u_1+6)$$

u_1, u_2 = Function of m, λ

The computer model was used to determine the pathlength for the sensor which would achieve greatest precision at a concentration of 4% CO2. This was accomplished by substracting the sensitivity as defined in Equation 2 of the sensor at a level of 3.9% CO2 from the sensitivity at a level of 4.0% CO2. This result as a function of pathlength is given in Figure 5. The optimal pathlength for highest precision at the 4.0% CO2 level is approximately 1 cm.

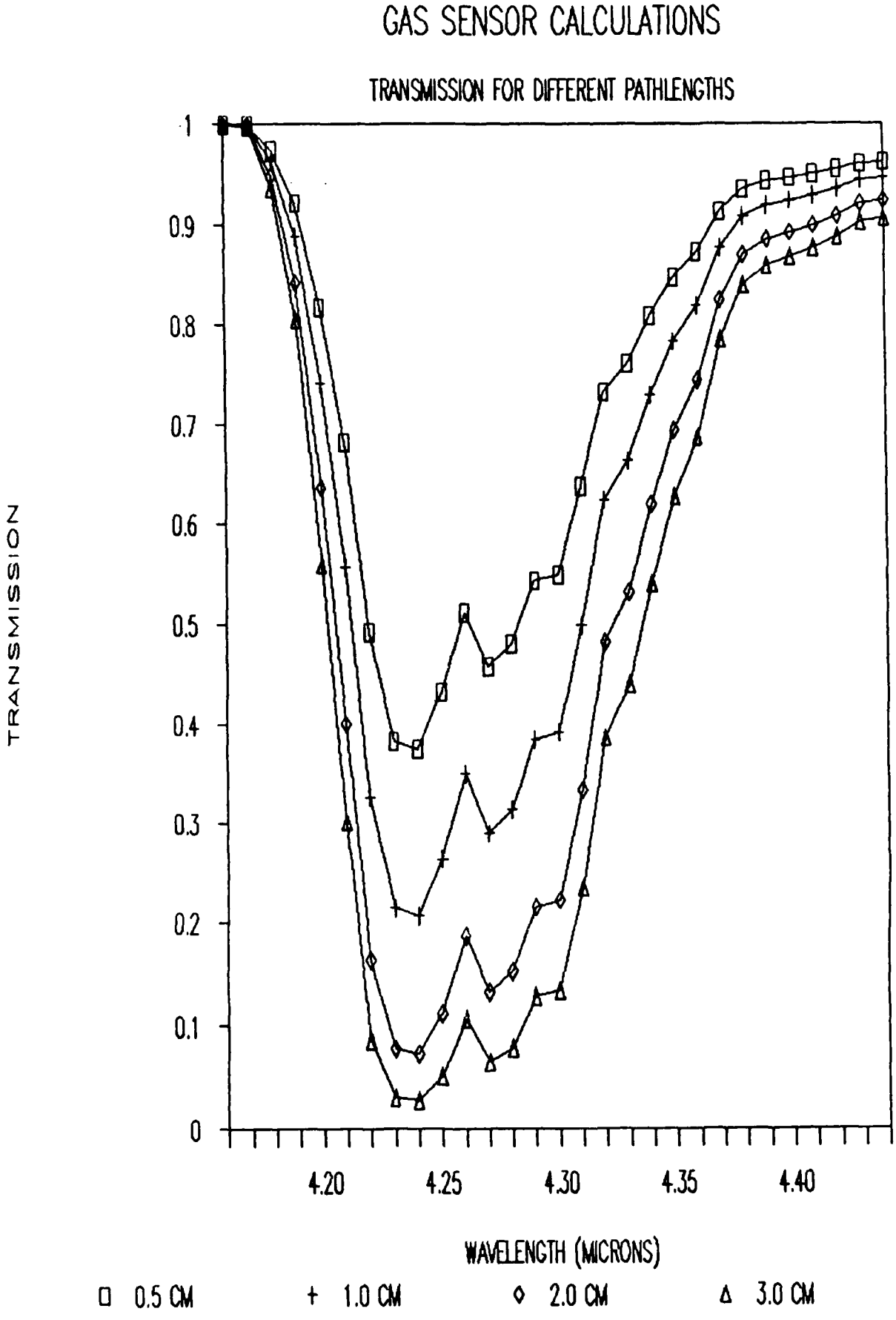

Figure 4. Carbon Dioxide Transmission vs Wavelength

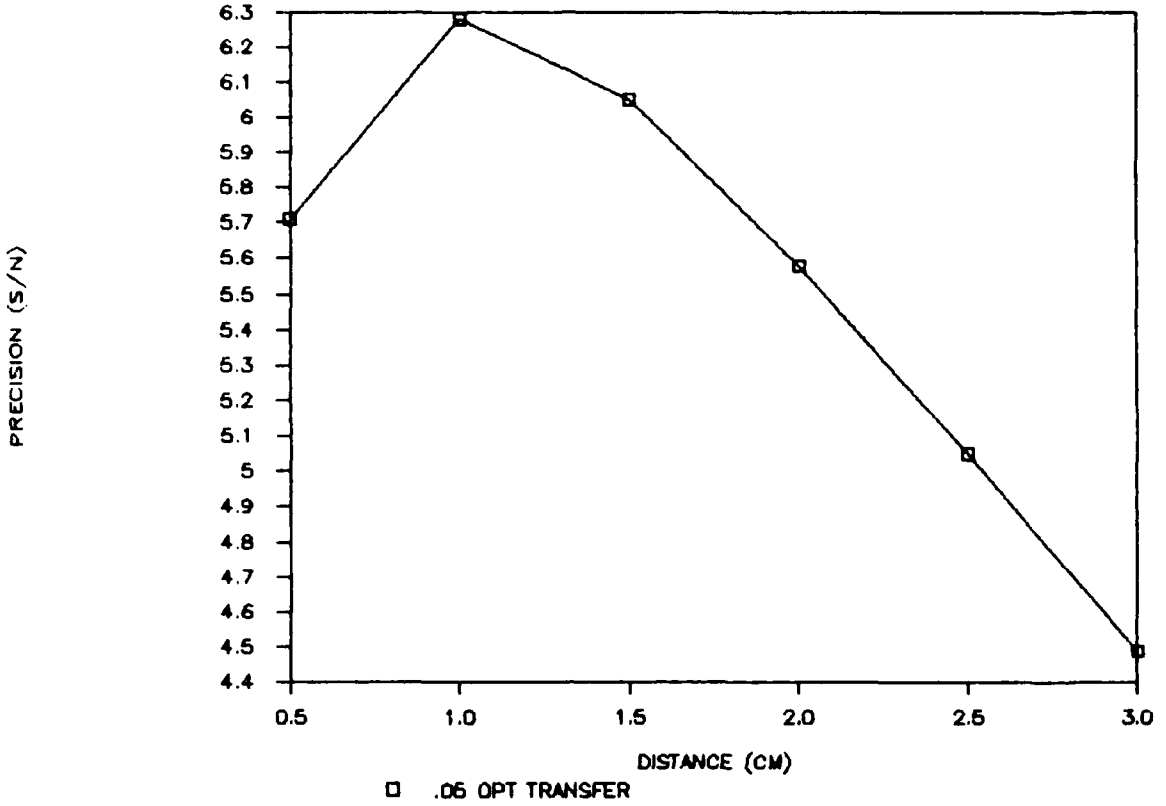

Figure 5. Sensor Precision vs Pathlength

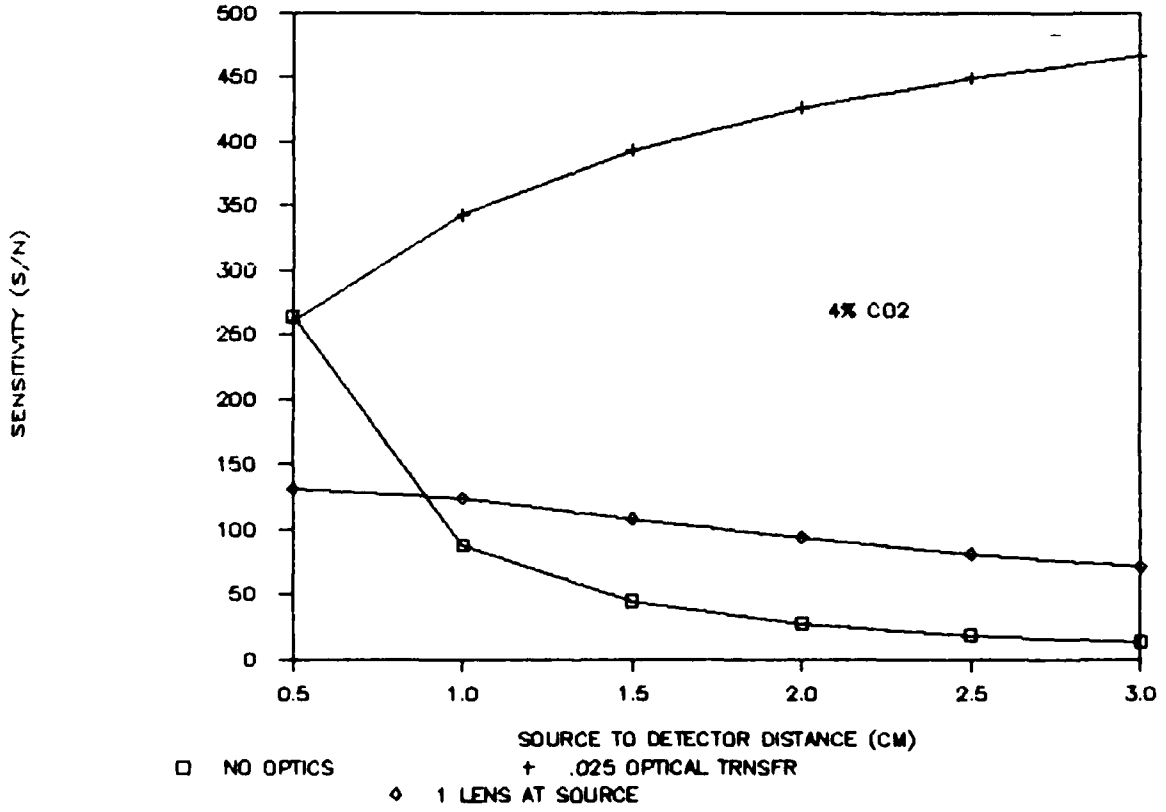

Figure 6. Sensor Sensitivity vs Detector Distance

The model was also used to evaluate the sensitivity of the system with selected optics. Figure 6 illustrates some of the calculations taken with no optics, a single spherical reflector acting as a collimator at the source and a constant .025 optical transfer from the source to the detector. Further results from the model are summarized in Table I.

The optical approach for the breadboard is illustrated in Figure 7. Reflecting plates were utilized to provide laminar flow in the sensing area and to provide some heat transfer to the windows, optics and filters. A refractive lens focuses the narrow (.051 cm) dimension of the source on the detector. The output from the wide dimension of the source is guided by the plates to the detector. A ray tracing of the optical path is provided in Figure 8.

A dual source was utilized within the sensor. One source was filtered for the carbon dioxide absorption band as shown in Figure 9, the other source was partially filtered. A PbSe detector with a single stage cooler was used to sense the modulated radiation. The miniature lens was fabricated from silicon.

Support electronics was fabricated for the sensor. This included a power supply, detector cooling control, source drive, preamplifier and post amplifier circuits. The output data from the source is captured by an Octagon 886 computer and data acquisition system. This data is then transferred to an IBM PC for data storing and graphics. A block diagram of the electronics utilized for the prototype is shown in Figure 10.

The source is modulated by a squarewave pulse at 2.3 KHz. The output of the source is focused on the detector. The detector output is amplified by a preamplifier with a gain of 500. An active filter follows the preamplifier inorder to reduce the noise out of the detector. The filter has a 3db bandwidth of 250 Hz. Further gain and rectification stages follow the filter. This is followed by a comparitor stage which allows adjustments for DC offsets and a final amplification stage.

The sensor was designed to fit within the opening of the hardshell of the pilot's mask. Various adaptors were designed. An extender to house electronics was also designed. An exploded view of the breadboard sensor design is provided in Figure 11.

The breadboard sensor had some anomalities. The dual source was fabricated inorder to conserve space, to minimize power and to have a capability to measure carbon dioxide absorption in different spectral regions inorder to compensate

TABLE I

MODEL PARAMETERS

Parameter	Units	Condition 1	2	3	4
Source Temperature	K	500	500	550	550
Detector Responsivity	V/Watt	16,500	33,000	16,500	33,000
Source Area	CM * CM		9.30E-03		
Delta Emissivity			1.50E-01		
Optical Transfer Coefficient			5.00E-02		
Path Length	CM		1		
Detector Noise	V/(SQ RT HZ)		4.70E-07		
System					
Bandwidth	Hertz		4.00E+02		
Noise	V		9.40E-06		
Sensitivity [1]		153	307	284	568
Precision [2]		1.40	2.80	2.60	5.19
Sensor Power [3]	Watts	1.58	2.28	1.92	2.57

1. S/N Ratio when sensing 4% CO_2.

2. S/N Ratio when sensing difference between 3.9% and 4.0% CO_2.

3. Assuming: A). .25 watts per cooler for 16500 V/watt and .90 watts for 33,000 V/watt responsivity,
   B). thermal resistance of source is assumed to be 150°C/watt for two source unit,
   C). losses in drive circuits not calculated,
   D). flow sensor power requirement not calculated.

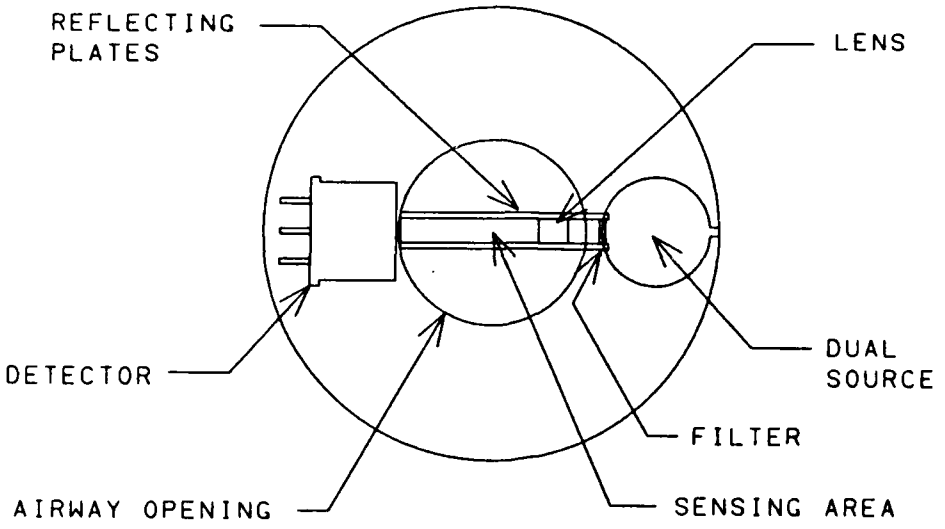

Figure 7. Breadboard Optics

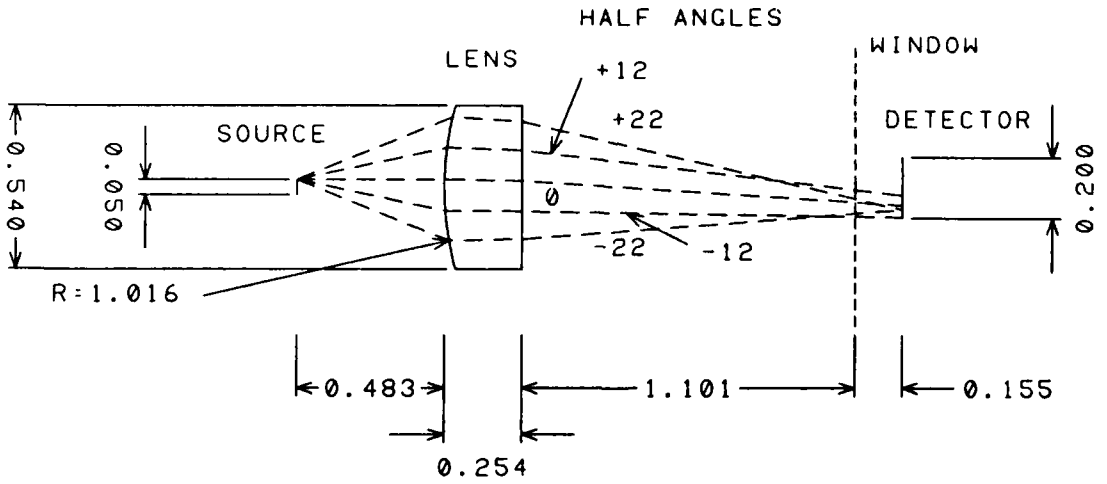

Figure 8. Breadboard Optical Raytrace
(all dimensions in cm or degrees)

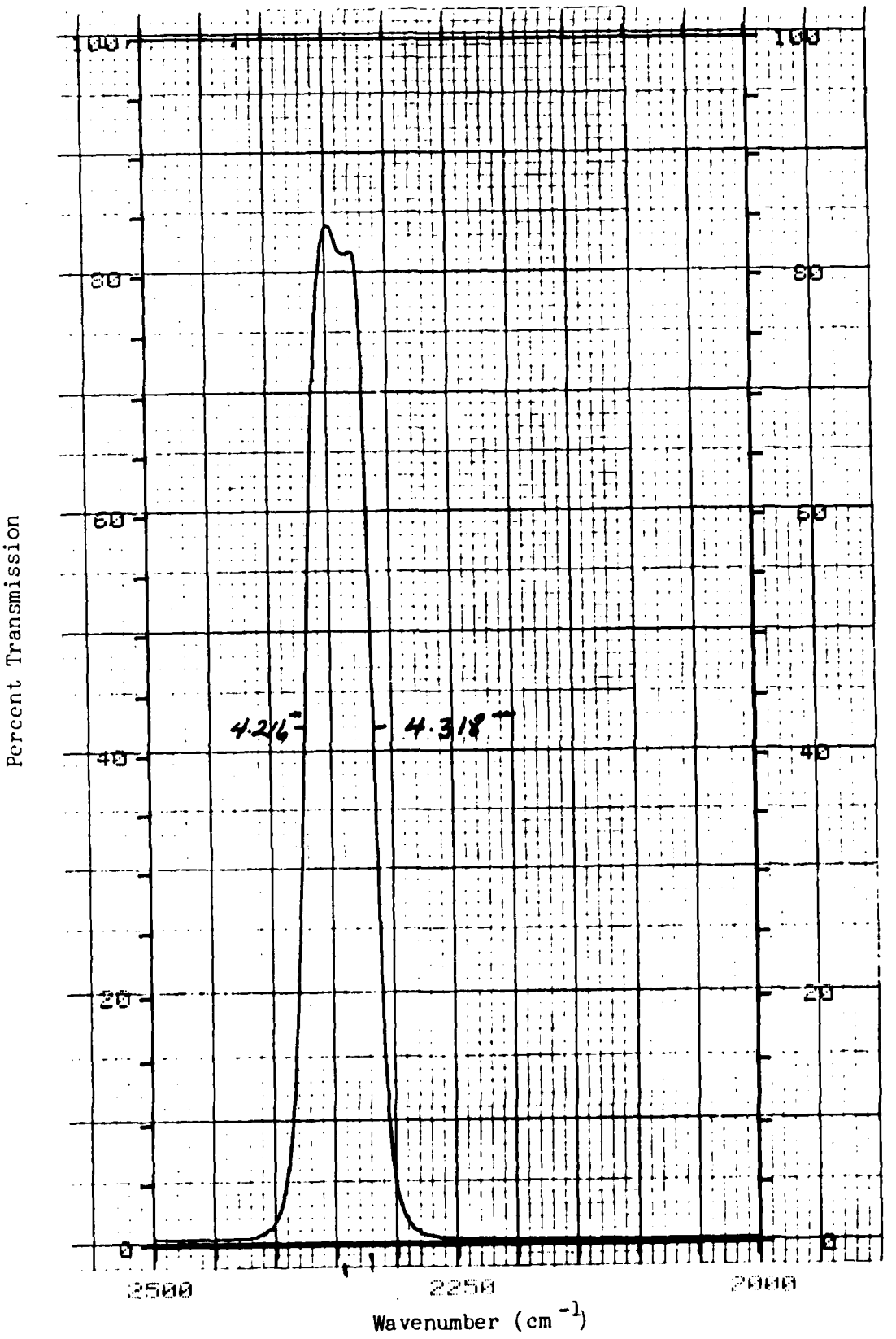

Figure 9. Carbon Dioxide Filter

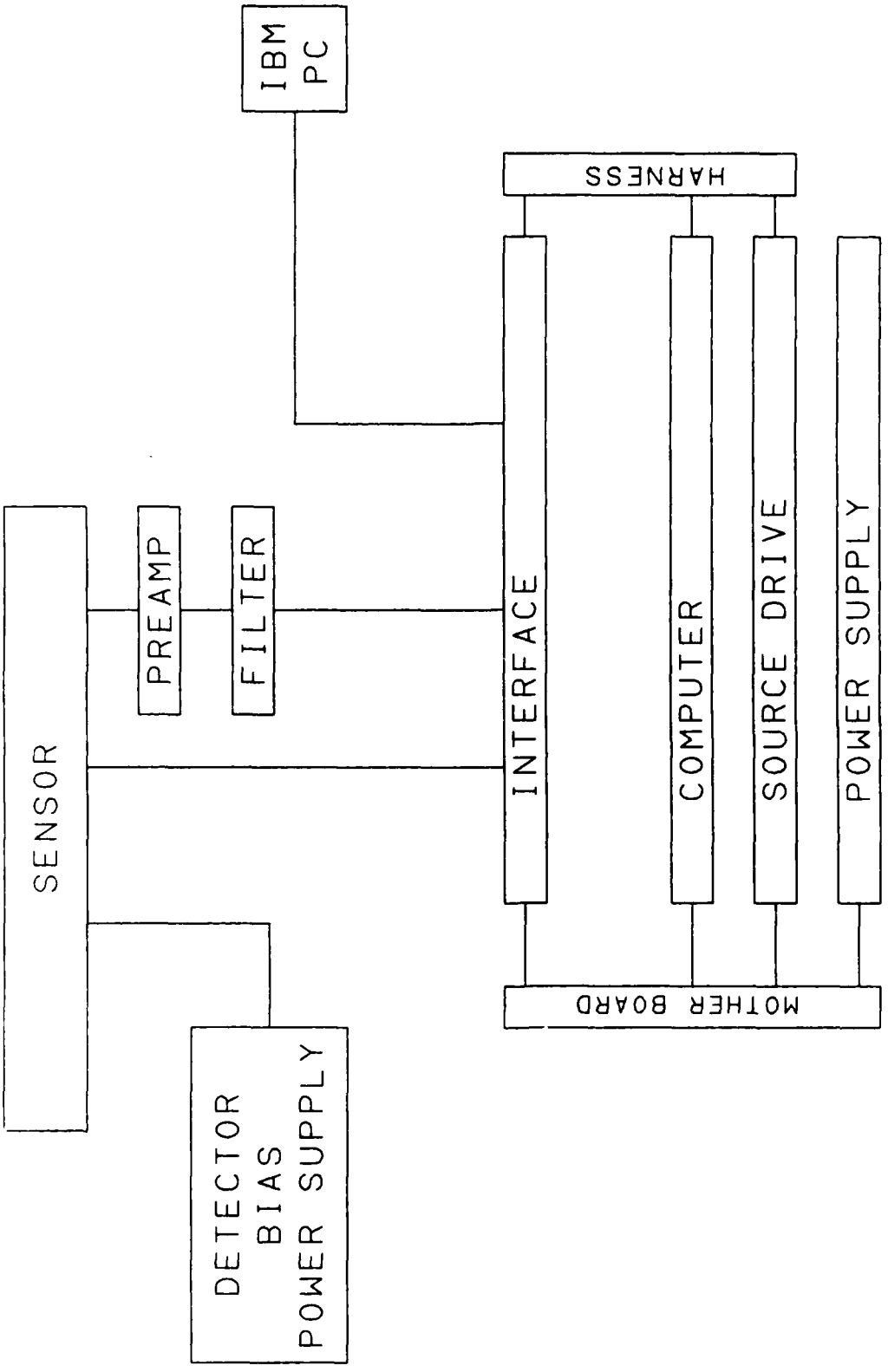

Figure 10. Prototype Electronics Block Diagram

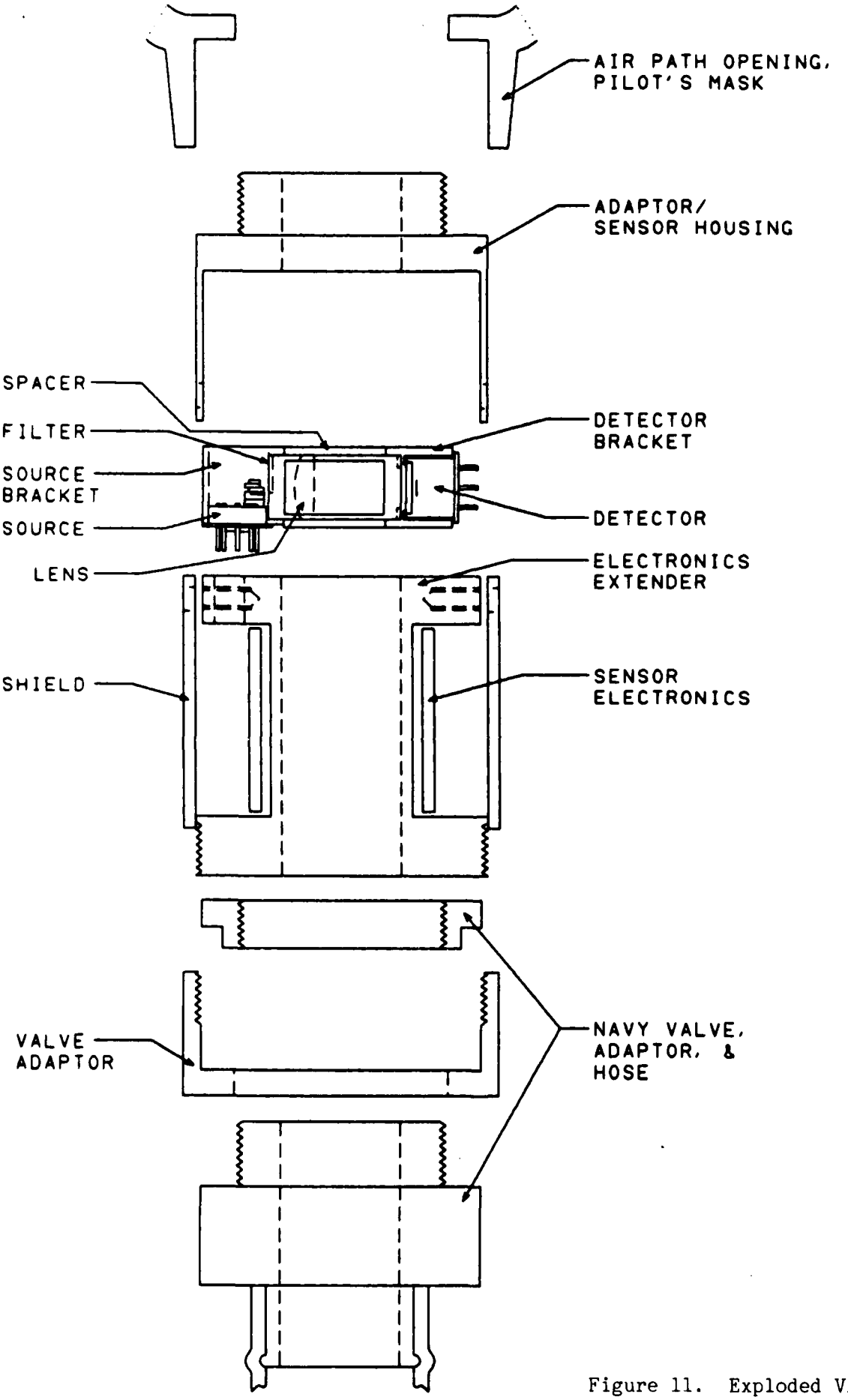

Figure 11. Exploded View of Breadboard Sensor Assembly

for and measure the effects of broadening of CO2 absorption due to oxygen and nitrogen. The dual source had problems which occured after installation in the sensor head. One source had a poor contact to the modulator and could not be used. Additionally, the temperature of the source was not being controlled. Data was taken, however, which could demonstrate the feasibility of the sensor concept. The data was taken with the source that was partially filtered. Improvements in assembly processes and techniques would eliminate the problems associated with the source.

A program was written for the Octagon 886 in ROBASIC inorder to gather data for testing in a breath by breath manner. The output of the sensor after gain and rectification was stored within the computer. Program execution time was approximately 8 milliseconds per data point.

A sample of initial data taken at 100 millisecond intervals is shown in Figure 12. The high signal levels are during periods when no carbon dioxide is present. During expiration the carbon dioxide lowers the signal levels. Upon inspiation the carbon dioxide is removed from the sensor. The data demonstrates the capability of the sensor to respond and take breath by breath data.

Further tests were taken with a data sampling time of 50 milliseconds per data point. The data is shown in Figure 13A. It is clear from the source temperature data that the inability to control the source temperature was affecting the signal output. The source was changing temperature dependent upon the flow of gas in the sensor as shown in Figure 13B. The source temperature data was used to normalize the output, this normalized output was then inverted inorder to produce a signal level that increases with increasing carbon dioxide concentrations shown in Figure 13C.

Prior to the above test 300 data points were analyzed in 100 data point increments inorder to determine system noise. The standard deviaion in the signal was .076, .072 and .074 volts for each of the 100 point increments. The difference in signal level with carbon dioxide present in the sensor and with no carbon dioxide during the breathing cycle was approximately 5 volts. This would provide a signal to noise (S/N) ratio of 67 for sensing 4% CO2. The S/N ratio could easily be increased. The partially filtered source was not optically aligned within the system and no antireflection coatings or reflective metalizations were applied to the lens.

The power dissipation of the breadboard sensor was measured and is tabulated in Table II. The sensor with preamplifier dissipates 1.87 watts. Over 50% of the power is consumed by the thermoelectric cooler of the detector, 40% is

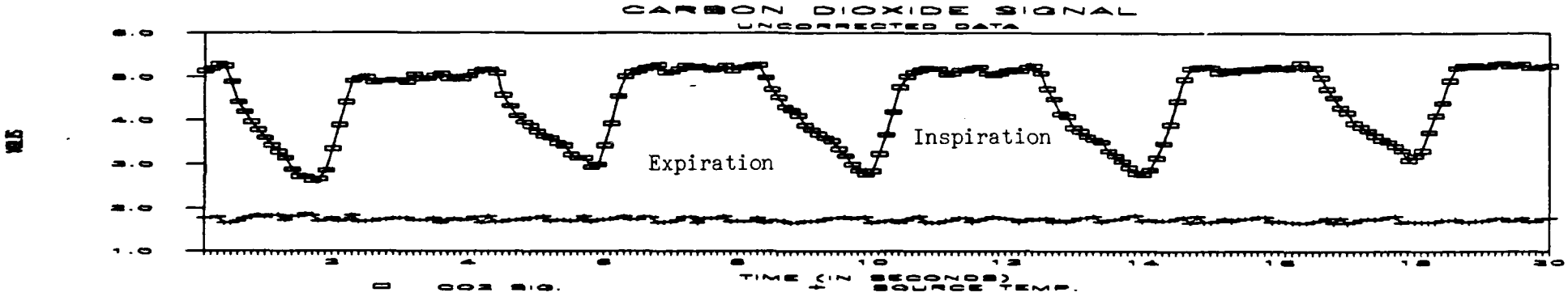

Figure 12. Breath by Breath Sensor Output
(100 millisecond intervals)

Figure 13A

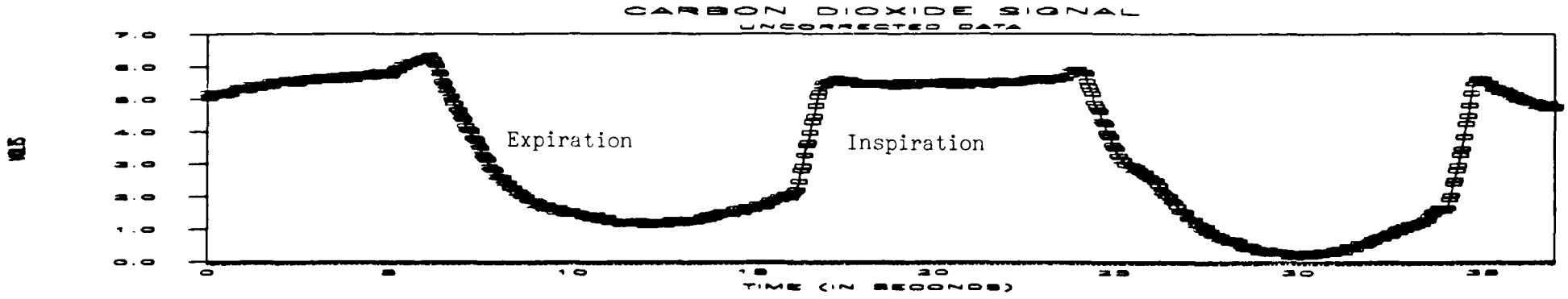

Figure 13B

Figure 13C

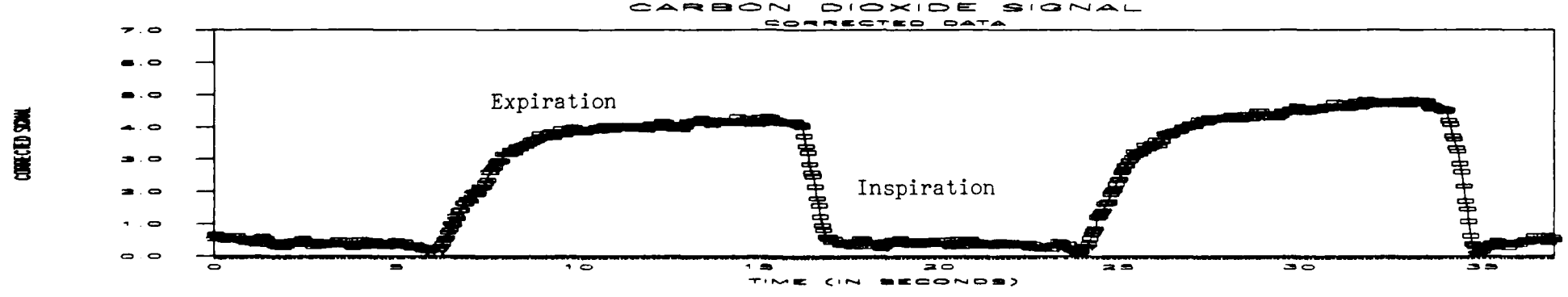

Figure 13. Breath by Breath Sensor Output
(50 millisecond intervals)

consumed by the source heater. Improvements in optics (antireflection coating of the lens) would provide more power to the detector and allow its' operation at a higher temperature which would reduce cooler power requirements. A factor of two gain in optics would allow the cooler power to be cut to .25 watts. Some of the power reduction would be offset by the requirement to heat optics to reduce condensation, the power losses in the drive circuits and the power requirements of the flow sensor.

Table II

Sensor Assembly Power Dissipation

Function	Power Dissipation (Watts)
Detector Bias	.004
-15V	.035
+15V	.034
Thermistor	.008
Cooler	.994
Source Heater	.757
Source Modulator 1	.001
Source Modulator 2	.037
Source Sensor	.001
	1.871

Since the source and detector reach their operating temperatures in relatively short time periods and temperature sensors are available to monitor their respective temperatures power could be reduced by operating the sensor only when triggered by an external signal. It may be necessary, however, to maintain heater power on the optics to prohibit condensation even when the source and detector are not operating.

Calculations were completed to illustrate the response characteristics of the sensor due to large changes in carbon dioxide levels. The calculations were completed with two estimates of source filtering or blockage. These are quantified in terms of a percent transmission outside of the optical filter passband. The results of these calculations are provided in Figure 14. Observations of the Figure show that the precision of the sensor will decrease at high concentration levels.

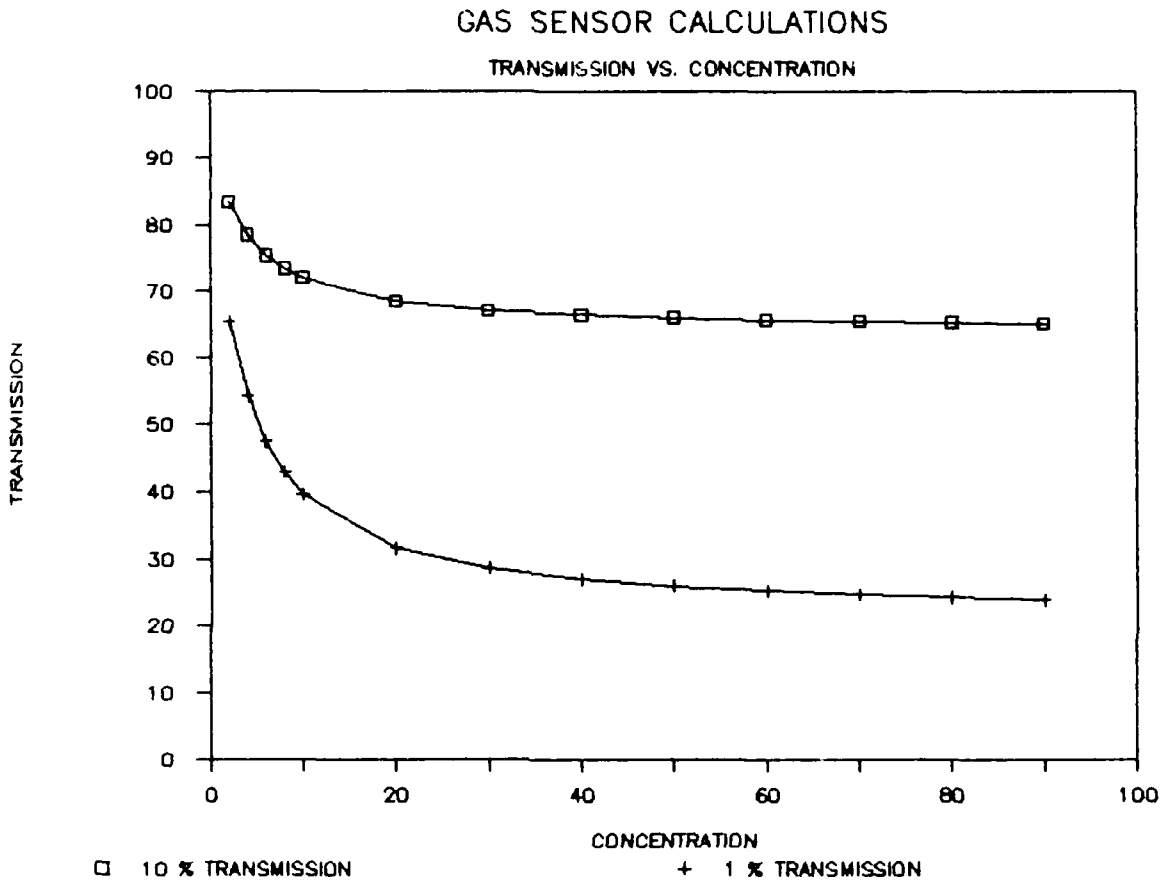

Figure 14. Sensor Transmission vs Concentration (For Two Different Transmission Outside of Filter Passband)

Tests were also conducted with the sensor system to determine its' susceptibility to changes in humidity and temperature levels. These tests were conducted prior to the breath by breath measurements and the source temperature control was operating appropriately. A room temperature gas dry inspiration cycle was followed by a hot, wet gas expiration cycle. Wet gas was obtained by bubbling room temperature dry gas (O2 or N2) through a heated water bubbler. These tests are summarized in Table III. One hundred percent attenuation was obtained when gas bubbled through 53°C water entered the sensor. However, when the test was repeated with additional heating of the sensor there was no attenuation. When gas was bubbled through 37°C water an attenuation of 6 - 9 % in signal level was obtained. The tests indicate that some additional heating will be necessary in the sensor to avoid condensation.

Table III

Moisture Temperature Tests

Test	Wet Expiration Temperature	Sensor Heating	Attenuation
1	53°C	None	100%
2	53°C	External Heating	0%
3	37°C	None	6-9%

Evaluations were made of a flow sensor utilizing a thermal chip being heated with constant power and a temperature sensor on the chip. The output of the temperature sensor was measured to indicate flow. Preliminary data was taken on the flow sensor which demonstrated that the device had a response time which would be unsuitable for a measurement of respiratory volume. The data shown in Figure 15A indicates that the sensor has approximately a .5 second response time. Figure 15B shows that with short breath pulses the sensor can barely respond.

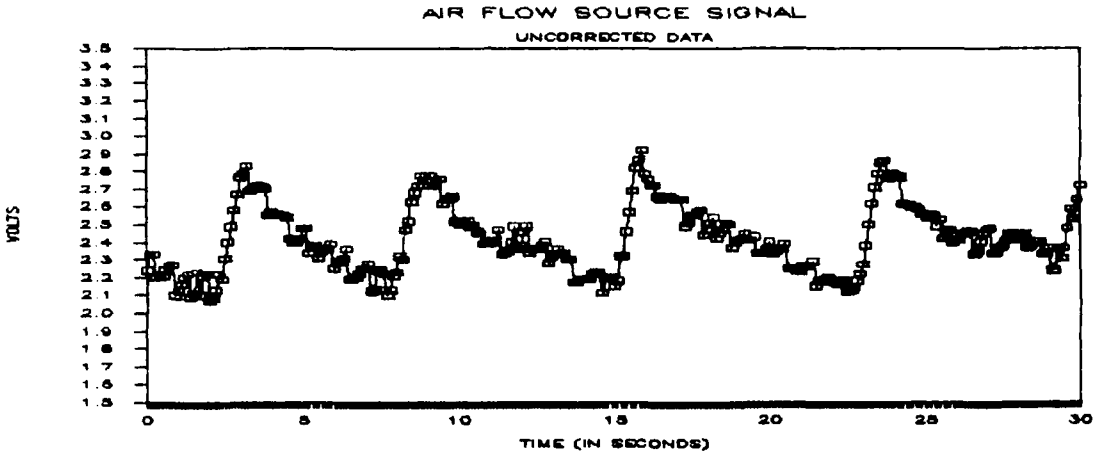

Figure 15A. Flow Sensor Response (Long Cycle)

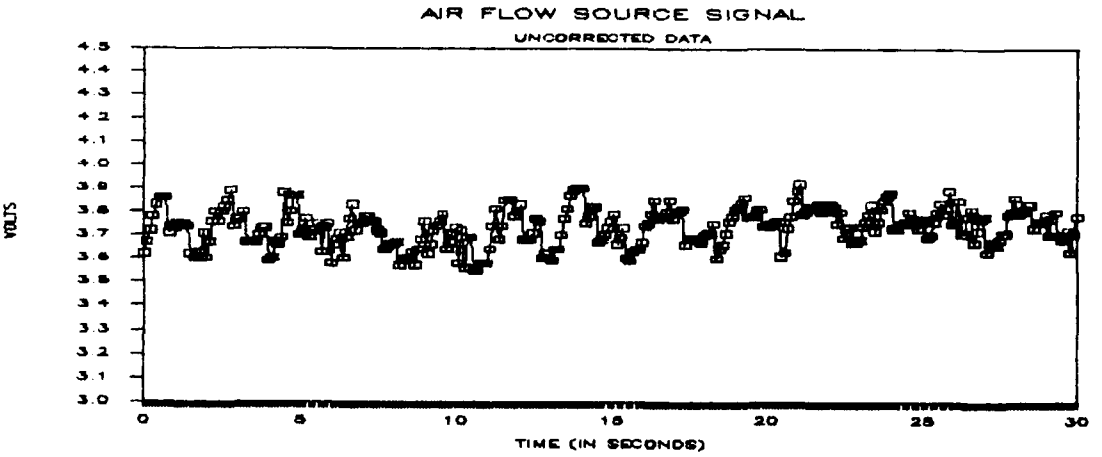

Figure 15B. Flow Sensor Response (Short Cycle)

III. BROADENING

Oxygen and nitrogen will change the absorption characteristics of carbon dioxide. Carbon dioxide will absorb more infrared radiation in the presence of nitrogen than in the presence of oxygen.

This effect was measured using the set up shown in Figure 16 inorder to determine if a wavelength region defined by interference filters could be found such that the difference in absorption characteristics could be used to measure the oxygen concentrations in the presence of carbon dioxide. The variable wedge filter shown in Figure 16 could be rotated to provide a continuously varying center wavelength with a bandwidth less then .15 microns from 2.5 to 8.0 microns.

Broadening measurements completed at 4.31 microns and 4.21 microns as a function of carbon dioxide concentration are shown in Figure 17. At 4.31 microns 2% carbon dioxide in oxygen was 5% less absorbing then 2% carbon dioxide in nitrogen. Similarly at 4.21 microns 2% carbon dioxide in oxygen was 2% less absorbing then 2% carbon dioxide in nitrogen. As the carbon dioxide concentration increased the broadening differences lessened. The small percentage difference in broadening and the variability with CO2 concentration would make it difficult to measure oxygen concentration over a short pathlength by relying on absorption coefficient differences due to broadening.

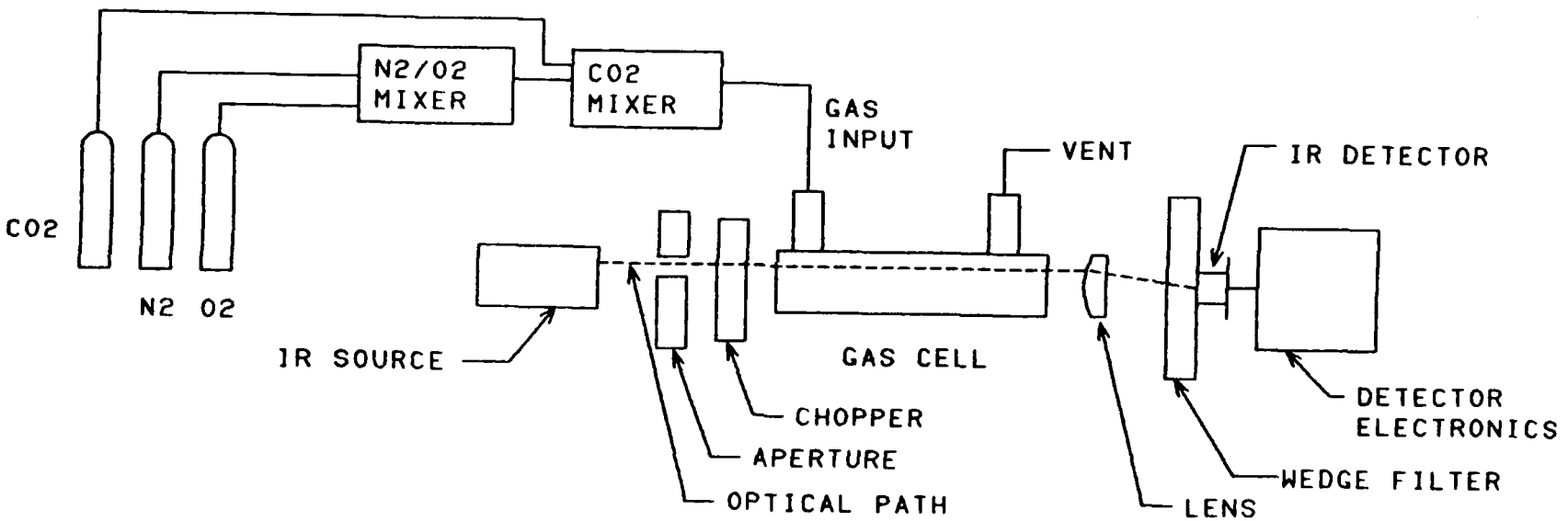

Figure 16. Broadening Measurement Set Up

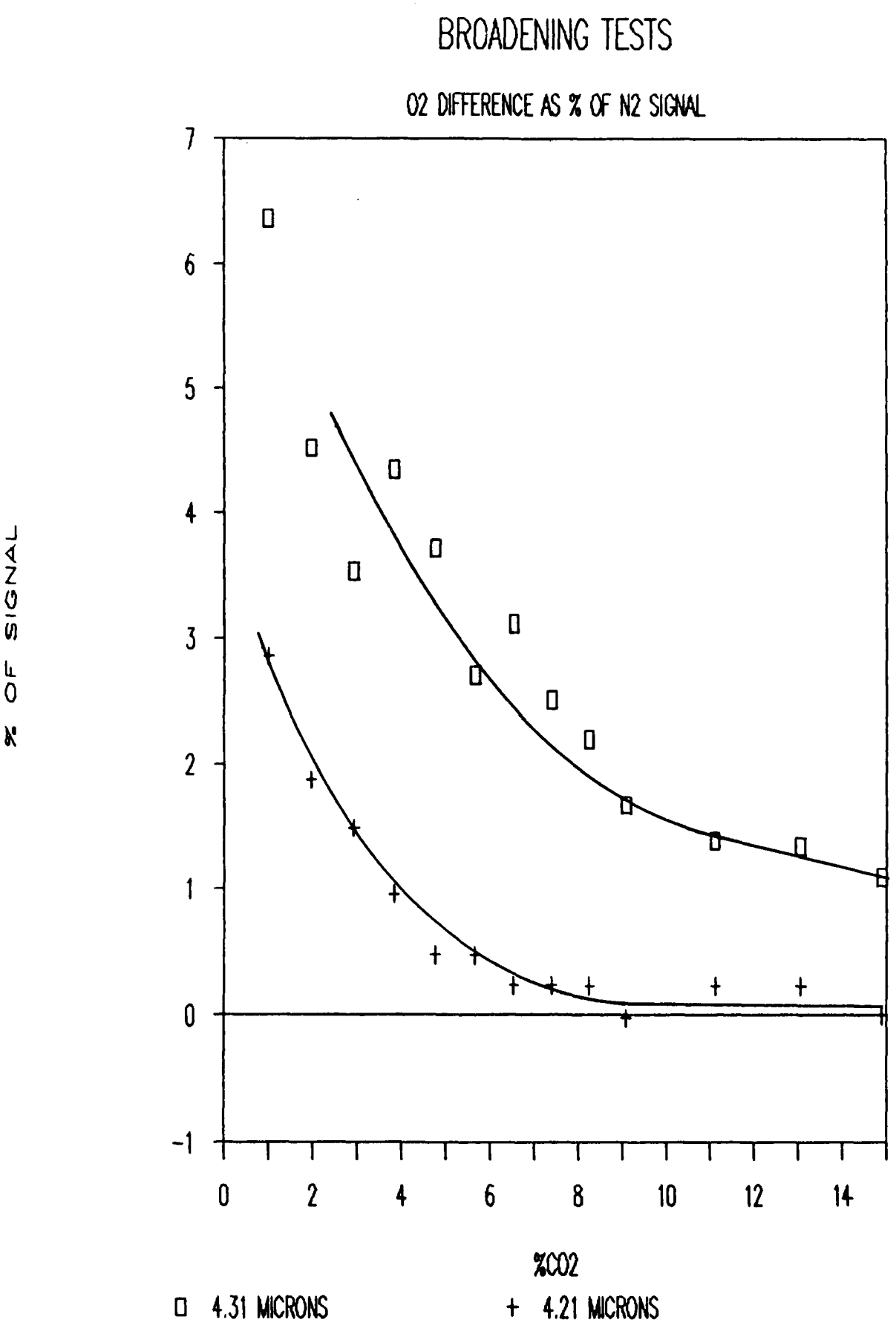

Figure 17. Transmission Differences Due to Broadening

IV. CONCLUSION

The objectives of the Phase I program were to

1). Determine if the proposed sensor will provide a breath by breath output suitable for the determination of metabolic function including data on
   a). respiratory rate.
   b). respiratory volume.
   c). carbon dioxide concentration.
   d). oxygen concentration.
2). Determine if the proposed sensor technology can be incorporated into the Naval aviator's oxygen mask including an analysis of
   a). location of sensor/sensors within mask extension.
   b). size and form of sensor necessary for incorporation in the mask to achieve desired sensitivity.
3). Determine if the proposed sensor technology can measure respiratory gases in the mask under simulated breathing considering
   a). abrupt changes in humidity of inspired/expired gases.
   b). abrupt changes in temperature of inspired/expired gases.
4). Determine if oxygen concentration can be sensed by measuring the carbon dioxide absorption broadening due to the presence of oxygen.

The data from the breadboard unit and the modeling have determined that the proposed sensor can provide a breath by breath output suitable for the determination of respiratory rate and carbon dioxide concentration. This sensor could easily fit within the extension of a pilot's mask and with suitable miniaturization the space allocated for the electronics in the breadboard unit could be significantly reduced. With additional heating the sensor would not be subject to abrupt changes in humidity and/or temperature of the inspired/expired gases.

Data taken on the broadening tests indicate that with a short pathlength sensor that the oxygen concentration cannot be effectively determined by measuring differences in broadening due to the presence of nitrogen or oxygen.

While the proposed approach for measuring respiratory volume did not have the speed of response necessary to provide a measure of respiratory flow there are still viable alternatives that include traditional "hot wire" sensors and fiber optic sensors. A hot wire sensor could be produced that would fit within the mask extension, however, it will require additional power. A flow sensor utilizing a fiber optic that would deflect with flow could also fit within the pilot's mask extension. This sensor would require minimal power but would need to be normalized for the g forces that would be encountered in the aircraft environment.

V. RECOMMENDATIONS

The sensing system depicted in the block diagram in Figure 18 is recommended. The sensor assembly would contain one EKLP source, the lens, filter and other optics, a cooled PbSe detector and preamplifier. The sensor would be designed to couple heat from the source and detector cooler to the optics where practical. The sensor assembly would also contain an auxiliary heater to avoid condensation of the optics. The flow sensor and preamp would also be contained within the sensor assembly.

External to the sensor assembly within a portable electronics package would be the source modulation, detector temperature control, source temperature control, signal filter, amplifier and power supplies. A power control switch would control power to the sensing system. The optics heater would bypass the power control. The system would sense carbon dioxide concentration and flow. The sensor assembly would connect to the mask and the hose in the same manner as the breadboard, however, it is estimated that the sensor assembly could be designed within approximately one half the length of the breadboard unit.

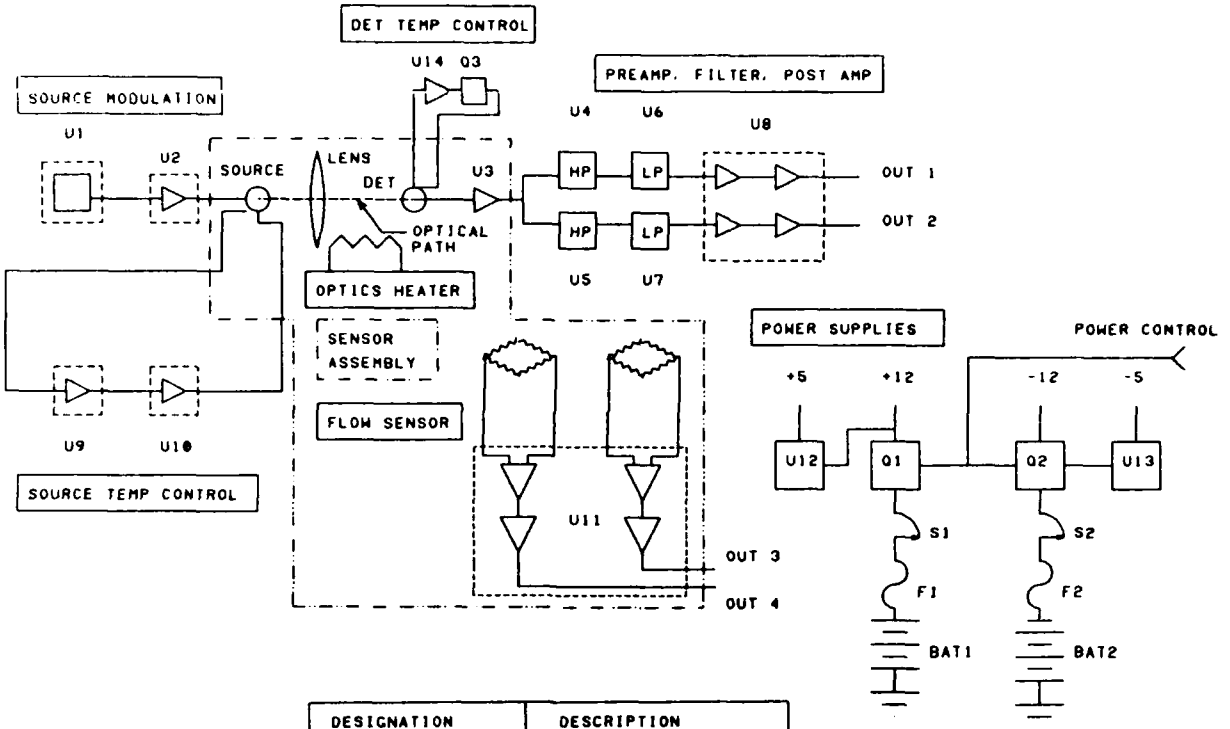

DESIGNATION	DESCRIPTION
U1	TIMER
U2	POWER AMP
U3	QUAD FET OP AMP
U4, U5	DIGITAL FILTER (HP)
U6, U7	DIGITAL FILTER (LP)
U8	QUAD OP AMP
U9	OP AMP
U10	POWER AMP
U11	QUAD OP AMP
U12	+5V REG
U13	-5V REG
U14	OP AMP
Q1, Q2	DARLINGTON AMP
Q3	POWER FET
S1, S2	SWITCH
F1, F2	FUSE
BAT1, BAT2	BATTERY
DET	IR DETECTOR
SOURCE	EKLP IR SOURCE

Figure 18. Recommended Sensing System

REFERENCES

1). Gas Analysis Instrumentation. A. Verdin, John Wiley & Sones, 1973.

2). "Techniques for Air Pollution Analysis", Gerald Rich, Pollution Engineering, Vol. 17, pages 43-44, June, 1985.

3). "Special Report on Air Toxics: Measuring and Monitoring", Paul N. Cheremisinoff, Pollution Engineering, Vol. 17, pages 21-29, June, 1985.

4). Infrared Spectra of Gases and Vapors Volume II- Grating Spectra. D. S. Erley, B. H. Blake, Dow Corning, March, 1965.

5). Hazardous Gases and Vapors: Infrared Spectra and Physical Constants. Brian Thompson, Beckman Instruments Technical Report 595, P/N 566665, August, 1974, Fullerton, California.

6). "New Solid State Infrared Source", Ralph M. Mindock, Proceedings of the 1987 SPIE Technical Symposium Southeast. May, 1987.

7). The Infrared Handbook Editors, William L. Wolfe, George J. Zissis The Infrared Information and Analysis (IRIA) Center, 1978.

END

DATE

FILM

DTIC

7—85